Journal of Great Lakes Research 35 (2009) 50–60

Contents lists available at ScienceDirect

Journal of Great Lakes Research

journal homepage: www.elsevier.com/locate/jglr

A hydrodynamic approach to modeling phosphorus distribution in Lake Erie

David J. Schwab [a,*], Dmitry Beletsky [b], Joseph DePinto [c], David M. Dolan [d]

[a] NOAA Great Lakes Environmental Research Laboratory, 2205 Commonwealth Blvd., Ann Arbor, MI 48105, USA
[b] Cooperative Institute for Limnological and Ecological Research, School of Natural Resources and the Environment, University of Michigan, Ann Arbor, MI 48109, USA
[c] LimnoTech, 501 Avis Dr., Ann Arbor, MI 48108, USA
[d] University of Wisconsin-Green Bay, 2420 Nicolet Dr., Green Bay, WI 54311, USA

ARTICLE INFO

Article history:
Received 22 January 2008
Accepted 25 September 2008

Communicated by Barry M. Lesht

Index words:
Lake Erie
Phosphorus
Modeling

ABSTRACT

The purpose of this paper is to show how a high-resolution numerical circulation model of Lake Erie can be used to gain insight into the spatial and temporal variability of phosphorus (and by inference, other components of the lower food web) in the lake. The computer model simulates the detailed spatial and temporal distribution of total phosphorus in Lake Erie during 1994 based on tributary and atmospheric loading, hydrodynamic transport, and basin-dependent net apparent settling. Phosphorus loads to the lake in 1994 were relatively low, about 30% lower than the average loads for the past 30 years. Results of the model simulations are presented in terms of maps of 1) annually averaged phosphorus concentration, 2) temporal variability of phosphorus concentration, and 3) relative contribution of annual phosphorus load from specific tributaries. Model results illustrate that significant nearshore to offshore gradients occur in the vicinity of tributary mouths and their along-shore plumes. For instance, the annually averaged phosphorus concentration can vary by a factor of 10 from one end of the lake to the other. Phosphorus levels at some points in the lake can change by a factor of 10 in a matter of hours. Variance in phosphorus levels is up to 100 times higher near major tributary mouths than it is in offshore waters. The model is also used to estimate the spatial distribution of phosphorus variability and to produce maps of the relative contribution of individual tributaries to the annual average concentration at each point in the lake.

Introduction

The establishment of the bi-national Great Lakes Water Quality Agreement of 1972 spurred the last major eutrophication management modeling effort in the Great Lakes. Aimed at controlling eutrophication in the Great Lakes, the governments of the U.S. and Canada implemented a program of phosphorus load reductions that was unprecedented in any region of the world (DePinto et al., 1986). Because of its high chlorophyll *a* concentrations and hypoxia in the central basin hypolimnion, Lake Erie received most of the attention with regard to developing a phosphorus load reduction strategy.

In order to develop a quantitative relationship between phosphorus loading and target water quality (summer average chlorophyll *a* and total phosphorus at spring overturn) in the lakes, a suite of models were developed and applied (Task Group III, 1978). In Lake Erie, these models (DiToro and Connolly, 1980; Chapra, 1977; Vollenweider, 1968, 1976) were applied to establish a target total phosphorus (TP) load that would achieve the water quality objectives of 15 and 10 μgP/L for TP and 3.6 and 2.6 μg/L for chlorophyll *a* in the western basin and central/eastern basins, respectively. For the central basin hypolimnion, the elimination of widespread hypoxia was also an objective. These models established a target total P load for Lake Erie of 11,000 MT/y. Because point source controls were not sufficient to achieve the target loads, best management practices were implemented on agricultural lands within the basin (DePinto et al., 1986) and by 1992, 34% of the Ohio Lake Erie basin land used for corn and soybeans was being farmed using conservation tillage practices (Ohio Lake Erie Office, 1993).

The target TP load for Lake Erie was first achieved in 1983 and annual TP load to the lake has fluctuated around that value since then. TP loads have varied plus or minus up to 3000 MT/y depending on the net basin water supply for a given year. Response to P load reductions was rapid, profound, and close to those predicted by DiToro and Connolly (1980). A post-audit of their eutrophication model indicated it predicted concentrations of P, chlorophyll *a*, and central basin hypolimnion dissolved oxygen quite well (DiToro et al., 1987). However, subsequent to the *Dreissena* invasion of Lake Erie that began in 1987, there has been evidence that the ecosystem of Lake Erie is processing nutrient loads differently, with special emphasis on the importance of nearshore processing and subsequent exchange with the offshore environment (Lam et al., 2006; Hecky et al., 2004). Unlike all previous eutrophication modeling efforts, this recent information calls for a much finer-scale quantitative analysis of the transport and

* Corresponding author.
E-mail addresses: david.schwab@noaa.gov (D.J. Schwab), dima.beletsky@noaa.gov (D. Beletsky), jdepinto@limno.com (J. DePinto), doland@uwgb.edu (D.M. Dolan).

0380-1330/$ – see front matter © 2009 Elsevier Inc. All rights reserved.
doi:10.1016/j.jglr.2008.09.003

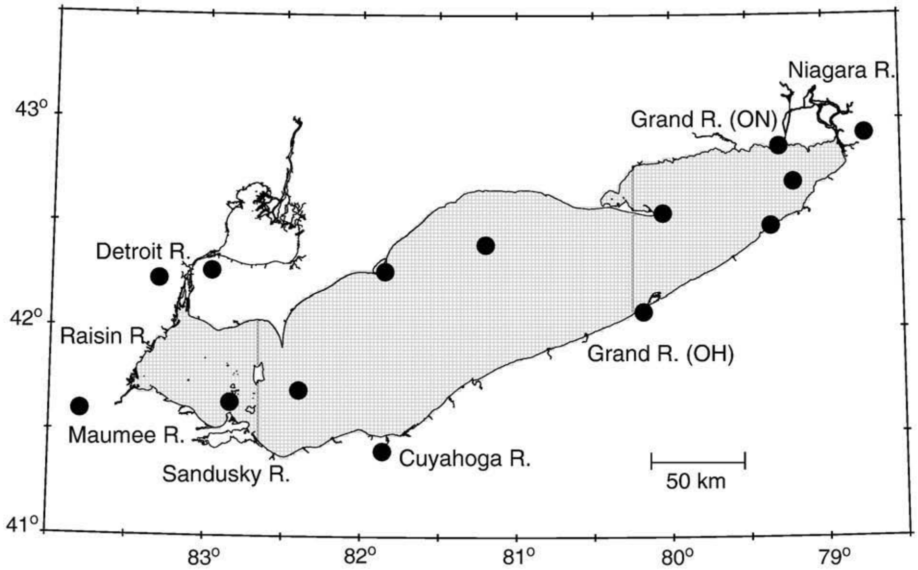

Fig. 1. Locations of major tributaries, locations of meteorological stations (filled circles), and depiction of 2 km computational grid used in 1994 simulations. Western, central, and eastern basins are separated by dark lines.

fate of nutrients that enter the lake via tributaries and direct runoff (León et al., 2005).

The purpose of this paper is to show how a high-resolution numerical circulation model of Lake can be used to gain insight into the spatial and temporal variability of phosphorus (and by inference, other components of the lower food web) in the lake. This exercise is also a necessary step toward the creation of a linked fine-scale hydrodynamic–eutrophication model which could be used to simulate conditions under a variety of loading scenarios. The calculations described in this paper are limited to a single year, 1994, in order to maintain focus on the spatial and temporal variability that can occur on sub-seasonal scales. Phosphorus loads to the lake in 1994 totaled 7736 MT, which is about 30% lower than the average loads for the past 30 years (11,000 MT). In fact, if we had selected a year with higher tributary flows and associated TP loads, the nearshore–offshore gradients we observed would have been even greater. We fully expect that the conclusions we draw about sub-seasonal variability by simulating the distribution of total phosphorus in Lake Erie during 1994 based on tributary and atmospheric loading, hydrodynamic transport, and net apparent settling would hold for other years as well.

Model formulation

The model developed for this application to Lake Erie has two components, 1) a hydrodynamic lake circulation model and 2) a phosphorus transport model. A 2 km horizontal grid was used to represent Lake Erie in the computations for both components. Lake currents were calculated in the hydrodynamic model using wind fields derived from the 14 stations shown in Fig. 1. Ice cover reported on twice-weekly National Ice Center ice concentration maps (Assel, 2003) was used to reduce momentum input into the lake when ice was present (January–April). The output from the hydrodynamic model was used to drive a simple total phosphorus model with a single *in-lake* TP sink term represented by a basin-dependent net apparent settling rate for TP.

The 3-dimensional hydrodynamic circulation model developed by Beletsky and Schwab (2001) is used to calculate circulation in Lake Erie. The model is based on the Princeton Ocean Model (Blumberg and Mellor, 1987) and is a nonlinear, hydrostatic, fully three-dimensional, primitive equation, finite difference model. The model uses time-dependent wind stress and heat flux forcing at the surface, free-slip lateral boundary conditions, and quadratic bottom friction. The drag coefficient in the bottom friction formulation is spatially variable. It is calculated based on the assumption of a logarithmic bottom boundary layer using constant bottom roughness of 0.1 cm. Horizontal diffusion is calculated with a Smagorinsky eddy parameterization with a multiplier of 0.1 to give a greater mixing coefficient near strong horizontal gradients. The Princeton Ocean Model employs a terrain following vertical coordinate system (sigma-coordinate). The equations are written in flux form, and the finite differencing is done on an Arakawa-C grid using a control volume formalism. The finite differencing scheme is second order and centered in space and time (leapfrog). The model includes the Mellor and Yamada (1982) level 2.5 turbulence closure parameterization. The hydrodynamic model of Lake Erie has 21 vertical levels (with equal spacing from surface to

Table 1
Total annual phosphorus loads and tributary flows for 1994 used in the model

Tributary	Total load (MT yr^{-1})	Average flow ($m^3\ s^{-1}$)	Avg. conc. ($\mu g\ l^{-1}$) (load/flow)
Detroit	3277	5712	18
Huron (MI)	31	18	55
*Raisin	110	17	205
Ottawa	31	6	164
*Maumee	1348	102	419
Portage	208	13	507
*Sandusky	308	28	349
Huron (OH)	115	6	608
Vermilion	112	6	592
Black	57	9	201
Rocky	59	9	208
*Cuyahoga	264	26	322
Chagrin	167	16	331
*Grand (OH)	159	25	202
Ashtabula	21	7	95
Conneaut	41	40	33
Cattaraugus	235	27	276
Buffalo	51	29	56
Grand (ON)	320	60	169
Big	29	14	66
Big Otter	74	14	168
Kettle	88	14	199
Total	7105	6198	

Daily flows and daily phosphorus concentrations were used for the tributaries marked with an asterisk. Other tributaries used daily flows, but with annual average concentrations.

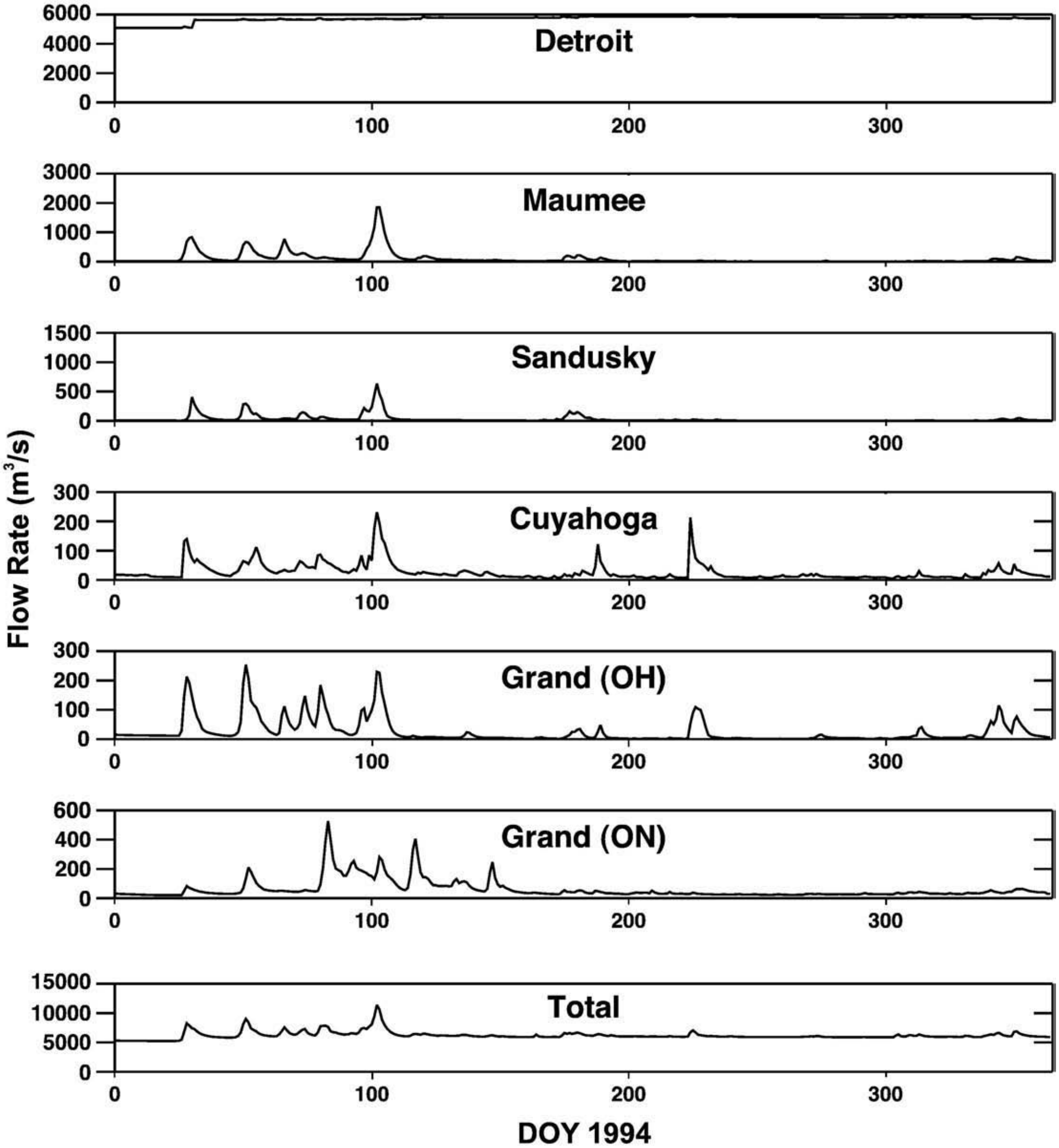

Fig. 2. Daily 1994 flow rates for selected Lake Erie tributaries.

bottom) and a uniform horizontal grid size of 2 km. Daily inflows from 22 tributaries and outflows at the Niagara River and Welland Canal were incorporated as boundary conditions in the hydrodynamic model (Table 1).

The phosphorus transport model uses the output currents from the hydrodynamic model to calculate the vertically averaged phosphorus concentration field (C) using the mass conservation equation:

$$\frac{\partial C}{\partial t} + u\frac{\partial C}{\partial x} + v\frac{\partial C}{\partial y} = S_{\text{in}} - S_{\text{out}} - \frac{wC}{d} \tag{1}$$

where u and v are the vertically averaged current velocities from the hydrodynamic model, S_{in} represents sources of phosphorus from tributaries and atmospheric deposition, S_{out} is the removal rate of phosphorus through outflows, w is a settling velocity, and d is depth. This equation is solved on the same 2 km computational grid as the hydrodynamics model using the numerical scheme of Bennett et al. (1983). The computational timestep is adjusted dynamically depending on flow conditions and is usually on the order of 20 min. The rationale for using the vertically averaged current velocities is that 1) river inputs to the lake are generally vertically mixed within a few kilometers of the river mouth, 2) the net horizontal transport in a shallow lake is mainly wind-induced. As shown theoretically by Bennett (1974) and confirmed experimentally by Saylor and Miller (1987), wind-induced net horizontal transport in Lake Erie is only weakly affected by stratification. Saylor and Miller (1987) found that measured currents in Lake Erie during both stratified and unstratified seasons agreed well with the results of the thermally homogeneous circulation model of Gedney and Lick (1972). They also point out that the main impact of stratification on horizontal circulation allows near-inertial vertically variable current motions which are out-of-phase above and below the thermocline and therefore have a negligible effect on net horizontal transport.

The 1994 total phosphorus loads for Lake Erie that are the basis for the loads used in Table 1 have been reported elsewhere (Dolan and McGunagle, 2005). Four source categories were used to develop these loads. Atmospheric loads are based on flux measurements obtained from Environment Canada (Chan et al., 2003) and applied to the surface area of Lake Erie. Direct point source loads (direct to the lake, downstream of sampling stations, or located in unmonitored areas) were estimated from effluent flow and concentration measurements. These data were obtained from the U.S. EPA's Permit Compliance System

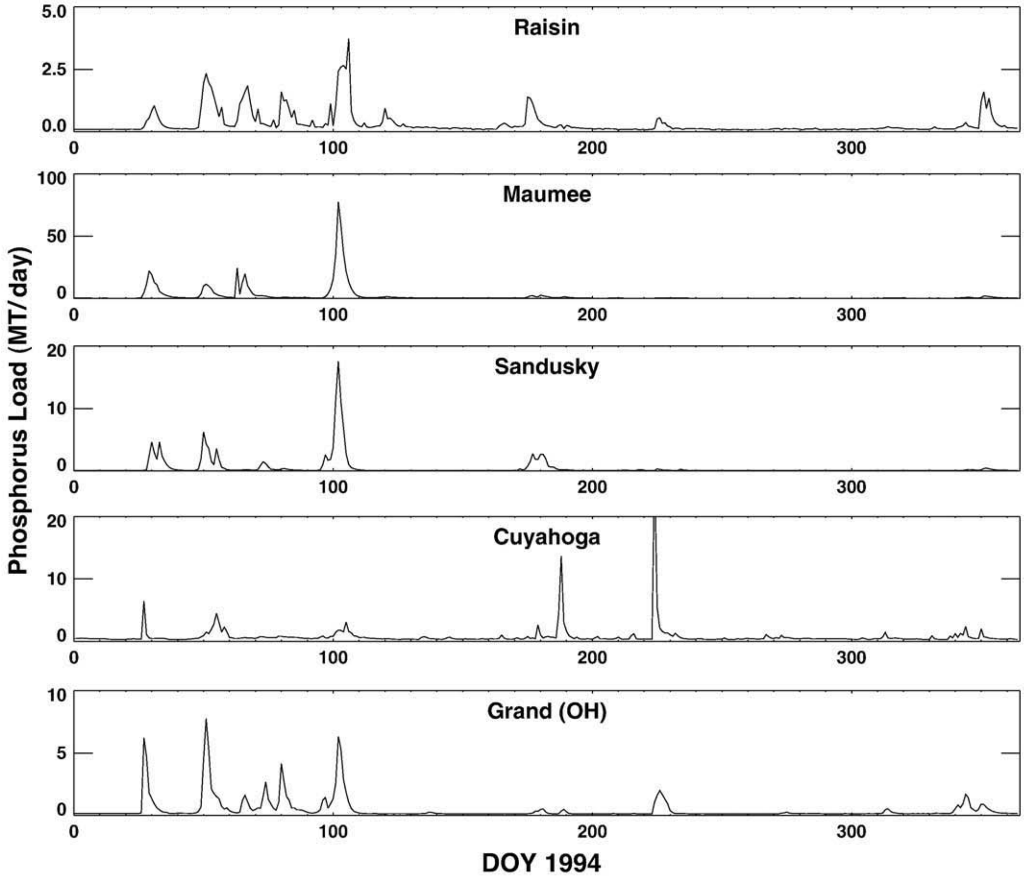

Fig. 3. Daily phosphorus loads for 1994 for 5 Lake Erie tributaries.

(PCS) database and the Ontario Ministry of the Environment's Municipal and Industrial Strategy for Abatement (MISA) database. See Dolan (1993) for more details. Monitored tributary loads were estimated using the Stratified Beale's Ratio Estimator (Beale, 1962; Tin, 1965; Dolan et al., 1981). Unmonitored areas were estimated using a unit area load (UAL) approach as described in Rathke and McCrae (1989).

Loads from Canadian and U.S. tributaries upstream of the mouth of the Detroit River, as well as from direct point sources, were included in the Detroit River load. Direct point source loads from other tributaries were added to the total of monitored and unmonitored tributary loads to arrive at the value in Table 1. All load estimates used were consistent with previously published estimates (Dolan and McGunagle, 2005) for all loading categories.

Daily flow rates for the 22 inflows were obtained from the GLERL Hydrologic Data data base (Croley and Hunter, 1994). These flows are based on USGS and Environment Canada, Water Survey streamflow records. Flows from some of the main tributaries, and the total of all tributaries are shown in Fig. 2. Daily phosphorus concentration values were available (or estimated) for five of the tributaries

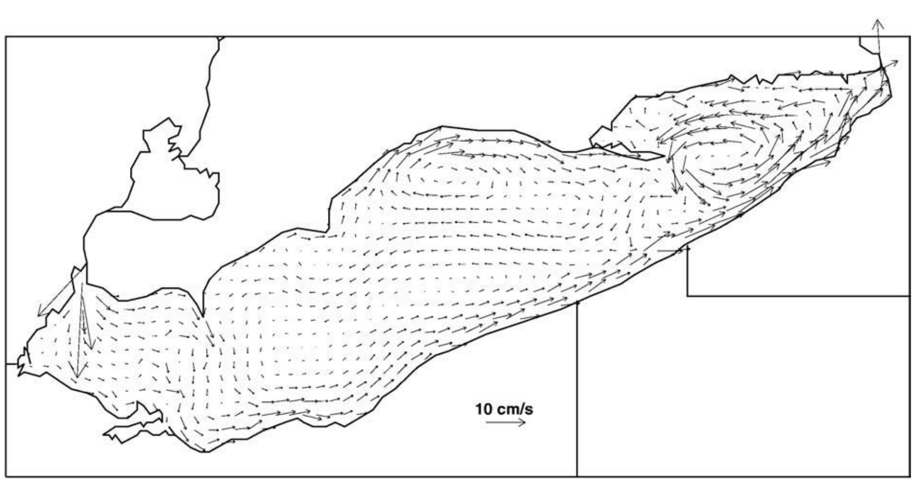

Fig. 4. Hydrodynamic model results showing Lake Erie average currents during May–October, 1994.

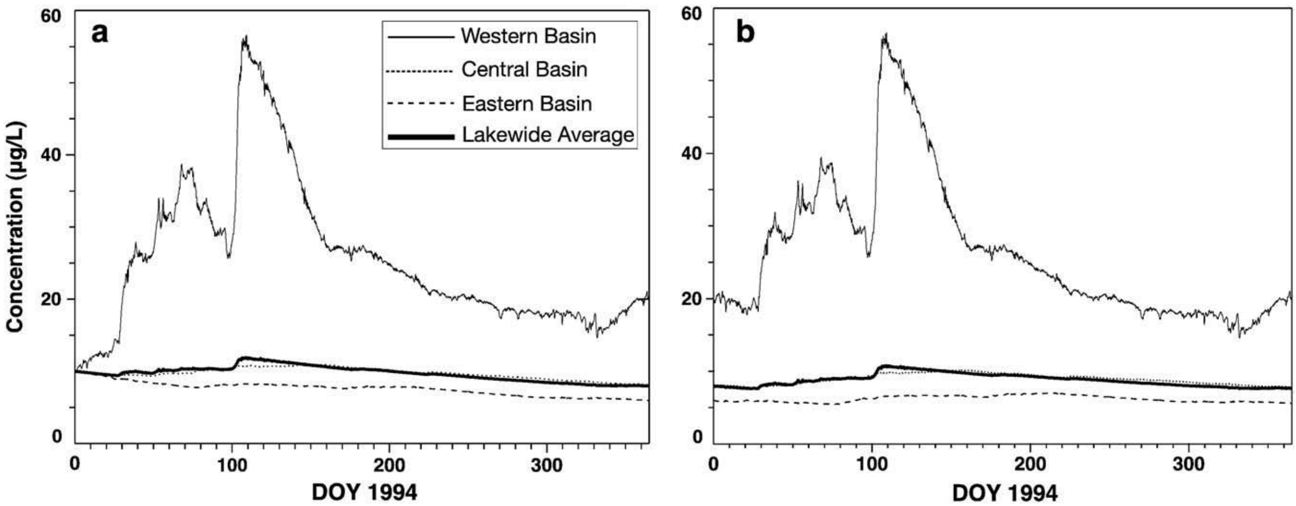

Fig. 5. Average phosphorus concentration by basin for run 1 (a) and run 2 (b). Thick solid line = lakewide average, thin solid line = western basin, dotted line = central basin, and dashed line = eastern basin.

(Raisin, Maumee, Sandusky, Cuyahoga, and Grand OH) from the Lake Erie Tributary Monitoring Program which is maintained by the Heidelberg College Water Quality Laboratory (Baker and Richards, 2002). Some daily concentrations for these tributaries were not obtainable due to logistical problems. For these samples, a stratified effective total phosphorus concentration was estimated using the Stratified Beale's Ratio Estimator cited above. The use of these estimated concentrations resulted in daily loads consistent with previously published estimates. Daily loads based on these values are shown in Fig. 3. For the rest of the tributaries, the daily flow rates were used to apportion the annual phosphorus load for each tributary into daily loads proportional to the daily flow rate, i.e. phosphorus concentration was assumed to be constant at the average value shown in Table 1.

Unmonitored and atmospheric loads were consolidated into a single 403 MT yr^{-1} source, which was entered as a uniformly distributed (in space and time) atmospheric load. The atmospheric load had little impact on the overall result and was mainly included for the mass conservation calculation. The Trenton Channel and Detroit River loads were consolidated and distributed 22/78 between the Trenton Channel and Detroit River.

Model results

The circulation model average currents for May–October of 1994 are shown in Fig. 4. The average currents are similar to those reported for 1994 by León et al. (2005) with eastward flow along the north and south shores of the central basin, a clockwise circulation gyre in the northeast part of the central basin, counterclockwise circulation in the eastern basin, and northwest to southeast flow in the western basin. The major difference is that the present results show a counter-clockwise circulation gyre in the southwest part of the central basin in agreement with available observations (Beletsky et al., 1999) while the results of León et al. (2005) show a clockwise gyre.

The total phosphorus transport model was initialized with a spatially uniform concentration of 10 μg l^{-1} on January 1, 1994. Tributary loads of phosphorus were delivered at the mouth of the tributary based on the daily load rate as described above. A basin dependent net apparent TP settling velocity was used. Following Lesht et al. (1991), the settling velocities chosen for the western, central, and eastern basins (as delineated in Fig. 1) were 3.17×10^{-7} m s^{-1} (10 m yr^{-1}), 7.29×10^{-7} m s^{-1} (23 m yr^{-1}), and 1.40×10^{-6} m s^{-1} (44 m yr^{-1}). These values reflect the long-term differences in biological uptake and internal recycling including annual average sediment resuspension within the three basins. The modeled average lakewide phosphorus concentration as well as average concentration by basin is shown in Fig. 5a. Calculations carried out with a single lakewide settling velocity were qualitatively similar for lakewide average concentration.

The transport model was then initialized with the concentration field from Dec. 31 and run again using currents from the 1994 hydrodynamic model run. The basin-wide average concentrations for the second year are shown in Fig. 5b. There is very little difference between the two runs outside of the first 25 days of the year. The phosphorus mass balances for the two runs are summarized in Table 2.

The mass discrepancies are due to using time-averaged transports and finite difference errors in the numerical advection scheme. The phosphorus transport model is very near steady-state by the end of the second year. To estimate the steady-state phosphorus concentration for the chosen combination of loadings ($S = 7104$ MT yr^{-1}), outflow ($Q = 6198$ m^3 s^{-1}), and TP net apparent deposition rate ($w = 8.15 \times 10^{-7}$ m s^{-1}), we can use a lakewide mass balance equation, i.e.,

$$\overline{C} = \frac{S}{Q + wA}. \tag{2}$$

Eq. (2) is the volume-integrated steady state version of the mass balance Eq. (1). For Lake Erie, the surface area A is approximately 25,800 km^2, so that $\overline{C} = 8.3$ μg l^{-1}, compared to modeled lakewide average concentrations of about 7.7 μg l^{-1} (Table 2).

Table 2
Phosphorus mass balance for the model run1 and run 2

	Run 1	Run 2
Tributary load (MT)	7104	7104
Atmospheric and unmonitored load (MT)	402	402
Total input (MT)	7507	7507
River outflow (MT)	1535	1291
Settling (MT)	6883	6290
Total output(MT)	8419	7582
Mass difference (MT)	912	74
Initial concentration (μg l^{-1})	10.0000	7.9541
Final concentration (μg l^{-1})	7.9585	7.6504
Mass difference (MT)	979	145

Comparison with observations

Phosphorus concentrations were measured during 7 NWRI cruises in 1994 (data courtesy of Murray Charlton, National Water Research

Table 3
Cruise dates, number of sampling stations, measured and modeled average phosphorus concentration for NWRI cruises in 1994

Cruise	Dates	Number of stations	Average concentration from samples (μg l^{-1})	Average concentration from model at sample points (μg l^{-1})
1	4/26–4/30	50	21	18
2	7/5–7/8	20	12	9
3	7/19–7/22	20	14	9
4	7/25–7/29	52	9	11
5	8/30–9/1	18	14	8
6	10/4–10/7	10	16	13
7	10/11–10/14	49	16	10
All	All		15	11

Table 4
Measured and modeled average phosphorus concentration by basin in 1994

Cruise	Western Basin			Central Basin			Eastern Basin		
	n	Obs.	Model	*n*	Obs.	Model	*n*	Obs.	Model
1	10	63	51	27	11	12	13	9	6
2				18	13	8			
3				19	14	9			
4	9	14	22	28	8	11	15	6	7
5				18	14	8			
6	5	18	18	5	14	8			
7	10	20	18	26	18	9	14	10	5

Concentrations are in μg/L.

Institute). It should be stated initially that the purpose of this comparison of our model with field observations is not for model calibration. Rather, the model-data comparison is intended to show that model results are within the general range of the observations and to provide insight into the behavior of the system with the intention of learning where the next step in model sophistication building should occur. If we had wanted to calibrate the model, we could have adjusted the TP net apparent settling and perhaps even modified it on a smaller temporal and spatial scale.

The dates for the 7 NWRI cruises are shown in Table 3. Station locations are shown in Fig. 6. If more than one sample was taken at a station, the mean value was calculated. At stations where samples were taken at a number of depths, the differences in concentrations at different depths were generally less than the differences from station to station. Average phosphorus concentrations for all stations during each cruise are compared with model results in Table 3. The modeled concentrations are generally lower then the observed values with an average difference of 4 μg l^{-1}. Not all cruises provided complete lakewide coverage. A comparison of modeled and observed concentrations by basin is shown in Table 4. The purpose of this comparison is to show that the modeled concentrations are within the observed range, and in fact most of the modeled average concentrations are within 5 μg l^{-1} of observed values. Correlations between observed and modeled concentrations are shown in Fig. 7. Modeled concentrations are generally comparable to observed values except for Cruises 5 and 7 where the modeled concentrations are consistently lower than observations. Two samples on Cruise 1 with values of 170 and 205 μg l^{-1} were considerably higher than all other observed concentrations. Outside of these measurements, there were no other samples with concentrations greater than 80 μg l^{-1}. The two high values were from stations 7 and 55 near the mouth of the Maumee River on 4/30 (DOY 120). This was shortly after the period of maximum discharge for the Maumee River. The maximum daily discharge rate of 1855 m^3 s^{-1}, about 1/3 the Detroit River flow, occurred on 4/13 (DOY 103). The concentration map from the model output on DOY 120 is shown below in Fig. 8.

From Fig. 8 it is clear that although the model was predicting only moderate concentrations at the two Maumee Bay sampling stations, there was an area of very high concentration just north of the sampling stations. In fact, just a day or two later the Maumee River plume moved southward in the model and produced high concentrations (>100 μg l^{-1}) at stations 7 and 55 (see time series plot in Fig. 9 below).

Time series plots of modeled phosphorus concentration at 10 of the sampling stations in Fig. 6 are shown in Fig. 9 along with the concentration values measured during the cruises. Stations 7, 55 and 56 are near the mouth of the Maumee River in the western basin of the lake. Stations 5, 28, 33, and 37 are in the central basin and stations 10, 15 and 18 are in the eastern basin. The modeled concentration at station 7 closest to the Maumee River mouth peaked at almost 1000 μg l^{-1} on day 105 when the discharge was at a maximum (see Fig. 2). A similar but shorter spike is seen at station 55, but station 56 has much lower values. As mentioned above, this is because lake currents were moving the Maumee River plume northward during this period. In the central basin (stations 5, 28, 33 and 37), modeled phosphorus concentrations are generally between 10 μg l^{-1} and 20 μg l^{-1} with higher values along the southern shore (station 37). The measured concentrations are close to the model values with the exception of a few points later in the year at stations 5 and 33. As discussed below, we believe this may be an indication of phosphorus resuspension during fall storms which is not included in the model at this time. In the eastern basin (stations 20, 15 and 18) concentrations are close to 10 μg l^{-1} except near the Grand River (ON) mouth

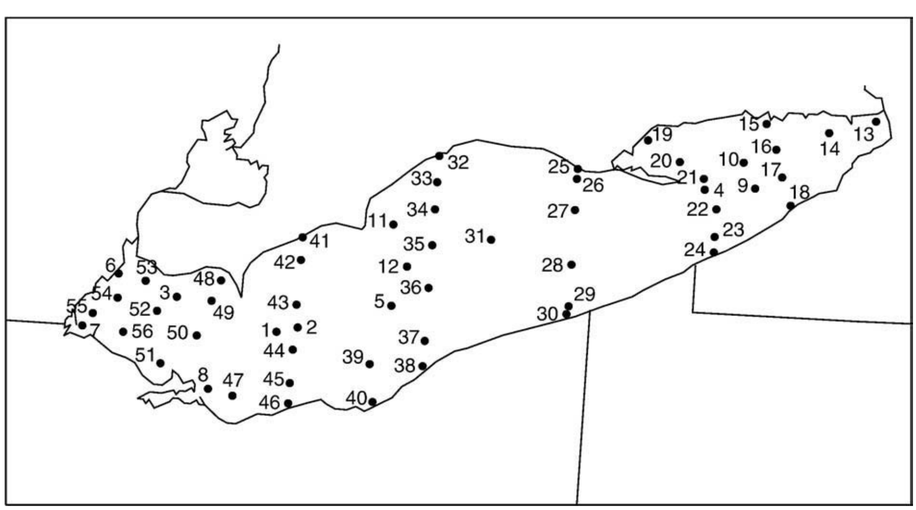

Fig. 6. Location of NWRI sampling stations in 1994.

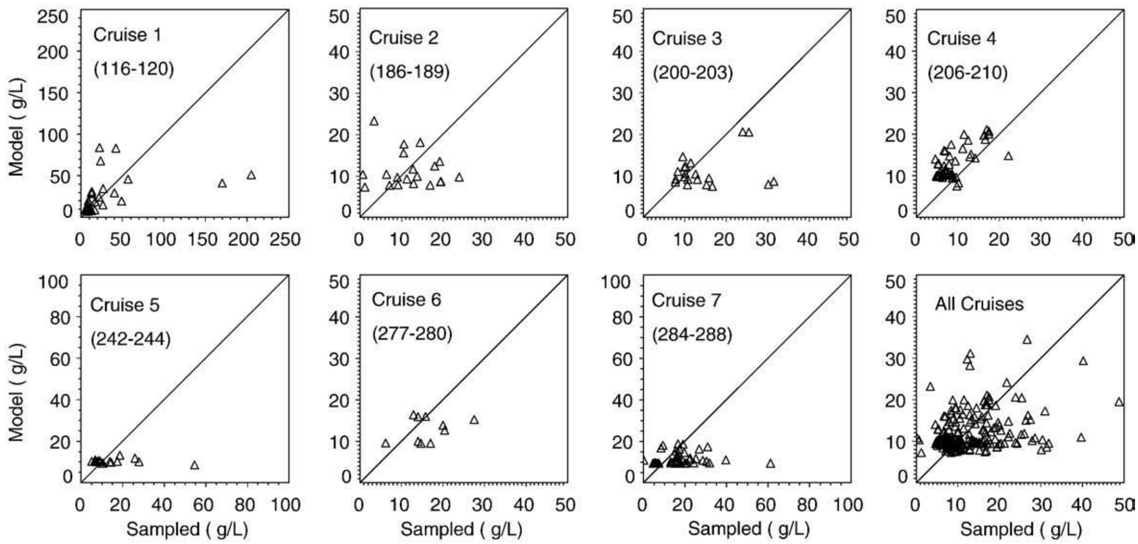

Fig. 7. Scatter plots of observed and modeled phosphorus concentration for each of the 7 NWRI cruises and for all cruises combined.

(station 15) where they are somewhat higher in the spring. Again, the observations are close to the model values, except for the single springtime measurement at station 15.

A map of the annual average phosphorus concentrations for 1994 is shown in Fig. 10. Average concentrations are highest near the mouth of the Maumee River (>100 μg l^{-1}) and exceed 10 μg l^{-1} along most of the southern shore. Average concentration at the Detroit River inflow is about 20 μg l^{-1}. Average concentrations in the north-central and eastern parts of the lake are generally less than 10 μg l^{-1}.

As an example of how this modeling exercise can be used to better understand the connection between lake circulation and phosphorus variability, a map of the standard deviation of the phosphorus concentration time series at each point in the lake is shown in Fig. 11. Most of the high variances occur in the western basin along the southern and western shores. The variance decreases near the mouth of the Detroit River. In the central basin, variance is about five times higher in the western part than in the eastern part.

Fig. 12 shows the coefficient of variation (variance divided by mean value) for phosphorus concentration in 1994. The highest coefficients of variation occur along the western shore of the western basin and at the mouths of the Portage River and Sandusky bay. There is an area of lower variability in the center of the western basin.

Another way the model can be used is to separate the contributions of individual tributaries to the annual average concentration in the lake. Four runs were made to determine the spatial distribution of the relative contribution to the annual phosphorus load from single tributary sources (Detroit R., Maumee R., and Sandusky R.) and from all tributary sources combined. This is done by eliminating the load from an individual tributary (or all tributaries for the fourth run) and

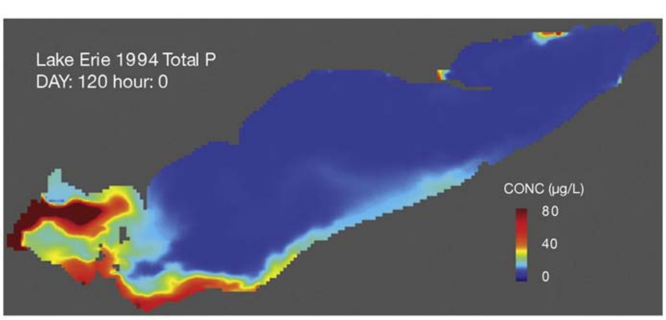

Fig. 8. Map of modeled phosphorus concentration on DOY 120, 1994.

then repeating the 1994 simulation. The relative contribution for that tributary is calculated by subtracting the resulting concentration fields from the average concentration map in Fig. 10 and dividing by the annual concentration. The result (Fig. 13) shows the percentage of phosphorus passing through each area of the lake, which can be traced back to a particular tributary.

The relative load contribution of the Detroit River (Fig. 13a) is over 50% in the northern part of the western basin but quickly drops to less than 15% in the center of the central basin. The highest contributions from the Maumee River (Fig. 13b) are along western and southern shores of the western basin. The influence of the Sandusky River (Fig. 13c) is mostly confined to the southern shore of the central basin east of the river mouth. Fig. 13d shows that the annual tributary load from all sources is greater than 50% in the western part of the lake and along the southern shore of the central basin and between 20 and 25% in the rest of the central basin.

Discussion and conclusions

The two-dimensional phosphorus transport model using daily tributary loads was shown to provide comparable phosphorus concentration values to the spatial and temporal distribution of phosphorus concentrations from the seven 1994 survey cruises. We see very high loads from all tributaries in the spring and to a certain extent in the fall, even though this was not a particularly wet year. These high flow tributary load events produced significant nearshore to offshore gradients in the tributary plumes, creating a source of high phosphorus concentration for nearshore nuisance algal growth to occur. The modeled lakewide average phosphorus concentration is close to the volume integrated steady state mass balance concentration. Spatially averaged phosphorus concentrations in the central and eastern basins show little temporal variability, although there are periods when concentrations near the tributary mouths are double or triple the lake average value. Because of its shallow depth and because it contains the largest tributary sources, the western basin shows considerably more temporal variability in average concentration. Peak spatially averaged average values are five times the lake average value for several days at a time and three times the lake average value for as long as two weeks during the spring runoff period. Local peak values near the mouth of the Maumee River can reach 100 times the lake average levels. We expect that the timing, magnitude and duration of the springtime maximum will change from year to year and, coupled with changes in the development of

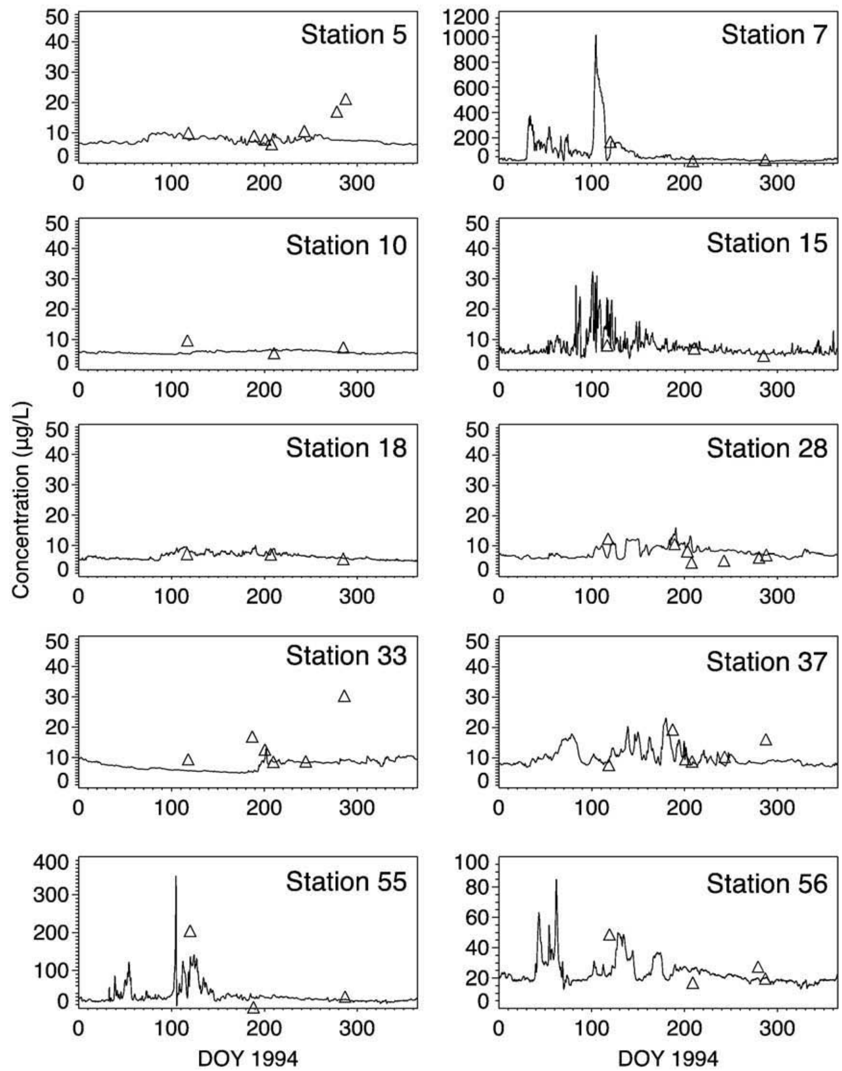

Fig. 9. Time series of modeled phosphorus concentration in 1994 at several of the stations shown in Fig. 4. Observed phosphorus concentrations are indicated by triangles.

thermal structure from year to year, will have considerable impact on the springtime plankton bloom.

The ratio of total phosphorus concentration to flow rate is higher in the late fall, winter, and early spring. This is especially true for the Maumee River. The Detroit River load is large and relatively constant in time and because of the large flow it is well-mixed relative to other tributaries. For all the other tributaries the high loads do not mix within the lake nearly to the extent to which the large box models

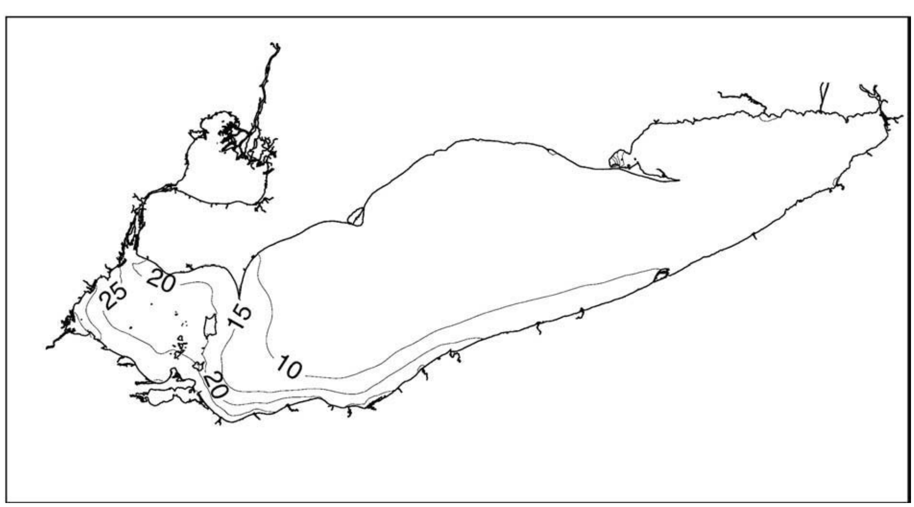

Fig. 10. Map of the modeled annual average phosphorus concentrations for 1994. Contours are at 10, 15, 20, 25, and 50 μg l^{-1}.

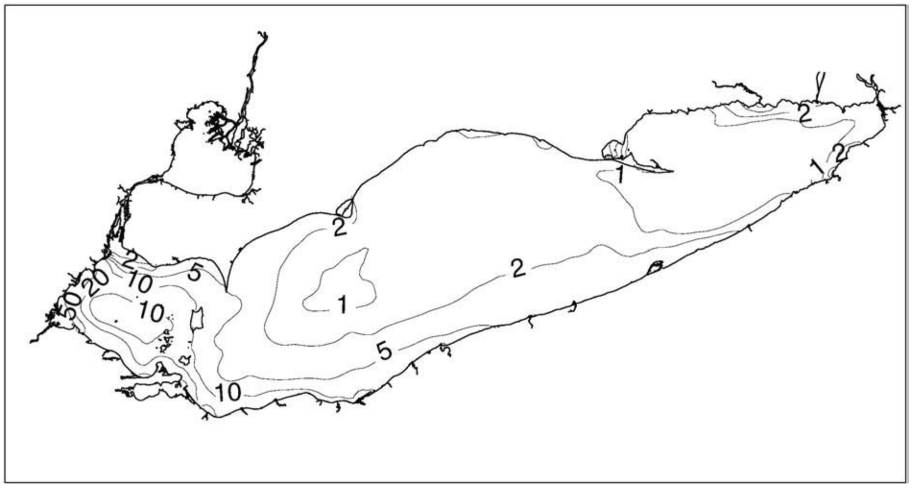

Fig. 11. Map of the modeled standard deviation of phosphorus concentration in 1994. Contours are at 1, 2, 5, 10, 20, and 50 μg l^{-1}.

would have them mix because of the large size of the segments and the completely-mixed assumption of the models. Because of the tendency for the Maumee and Sandusky plumes to "hug" the southern shore of the lake, they have a disproportional influence on the southern nearshore than elsewhere in the lake. Because the major loads enter the western basin, there is a tendency for higher P concentrations (and by extension higher phytoplankton growth and maybe even low DO) to move from west to east during the course of a year. The map of annual average concentration (Fig. 10) shows values up to 10 times the lake average levels near the mouth of the Maumee River in the western basin and average values as much as twice the lake average level extending eastward from the western basin along the south shore of the central basin well past the Cuyahoga River at Cleveland. There is also a zone of higher than average concentration in the northern part of the western basin that is related to the northward advection of the Maumee River plume. It will be interesting to see if this feature appears in other years, or if it is unique to 1994 conditions.

In summary, the main deficiencies of the model are the under prediction of phosphorus levels in the eastern part of the central basin in the fall and rather poor overall correlation with cruise data. The spread of points in comparisons with the cruise data is probably the result of lumping (time and space and kinetic averaging) of the TP dynamics in the model that is limiting its ability to capture short-term and small spatial scale events in the lake, such as short-lived and localized resuspension events. The low modeled concentrations in the fall are most likely due to resuspension of bottom material by waves, which is not included in the present model. This model does not capture episodic resuspension events because it only uses a constant net apparent TP deposition rate for each basin. It is also possible that the data are capturing sediment phosphorus diffusive flux induced by hypoxia. This is another localized process that the model is averaging and therefore cannot capture. While the basin-specific lumped parameter rates capture the net annual effect of internal phosphorus cycling, the effect of episodic resuspension and hypoxia can be included at the next level of model sophistication by separating the process into gross deposition and gross resuspension that can vary with time depending on environmental conditions. A further improvement can be made by adding a lower food web sub-model to account for water column phosphorus cycling. This paper represents just the first step toward a full 3D linked hydrodynamic–eutrophication water quality model for Lake Erie. We envision that a full 3D linked water quality model would ultimately be run at the same scale as the hydrodynamic model and would ideally contain not only a traditional lower food web model, but also a *Dreissena* sub-model to investigate of the potential impact of *Dreissena* on phosphorus cycling and transport from nearshore to offshore.

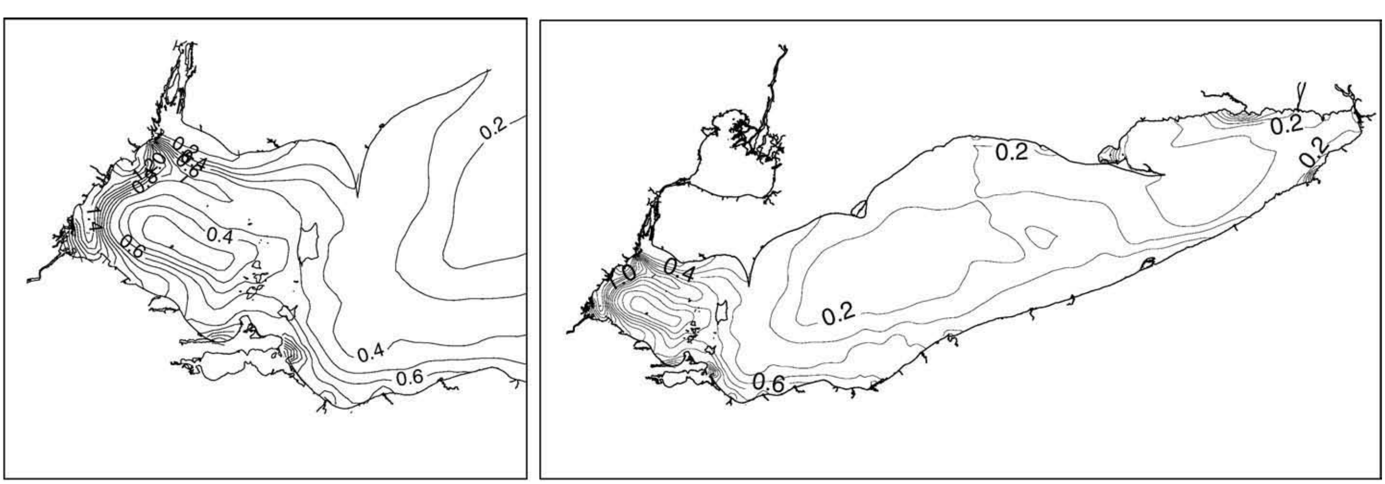

Fig. 12. Coefficient of variation (standard deviation divided by mean) for phosphorus concentration in Lake Erie in 1994. The contour interval is 0.1.

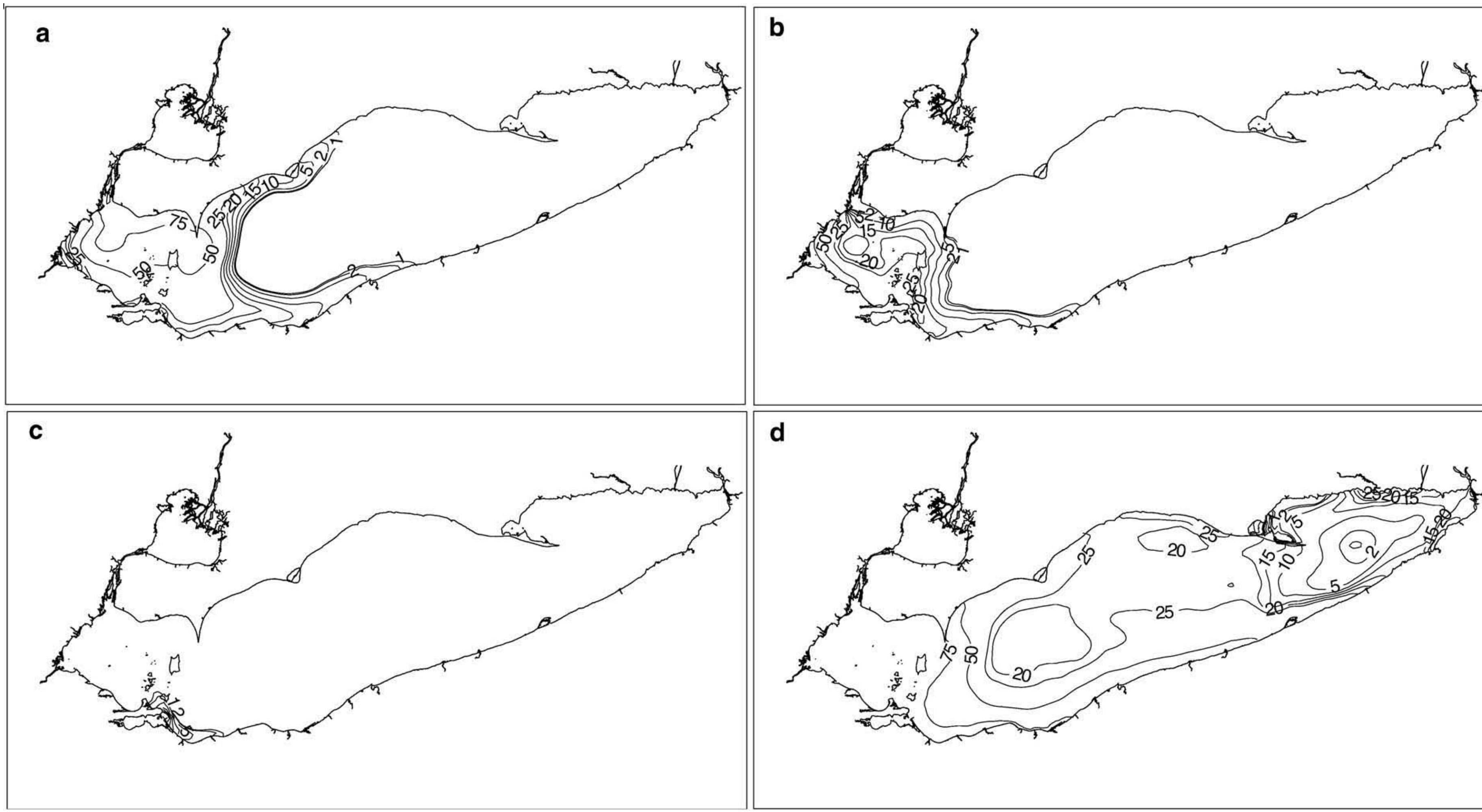

Fig. 13. Relative contribution to annual phosphorus load from (a) Detroit R., (b) Maumee R., (c) Sandusky R., and (d) all tributaries. Contour lines are drawn for 1, 2, 5, 10, 15, 20, 25, 50, and 75 percent.

Acknowledgments

We would like to thank Dr. Murray Charlton for providing the NWRI cruise data. This is GLERL Contribution number 1486.

References

Assel, R.A., 2003. An Electronic Atlas of Great Lakes Ice Cover. NOAA Great Lakes Ice Atlas, Great Lakes Environmental Research Laboratory. Ann Arbor, Michigan. 48105.

Baker, D.B., Richards, R.P., 2002. Relationships between changing phosphorus budgets and riverine phosphorus export in northwestern Ohio watersheds. J. Environ. Qual. 31, 96–108.

Beale, E.M.L., 1962. Some uses of computers in operational research. Ind. Organ. 31, 51–52.

Beletsky, D., Schwab, D.J., 2001. Modeling circulation and thermal structure in Lake Michigan: annual cycle and interannual variability. J. Geophys. Res. 106, 19745–19771.

Beletsky, D., Saylor, J.H., Schwab, D.J., 1999. Mean circulation in the Great Lakes. J. Great Lakes Res. 25 (1), 78–93.

Bennett, J.R., 1974. On the dynamics of wind-driven lake currents. J. Phys. Oceanogr. 4 (3), 400–414.

Bennett, J.R., Clites, A.H., Schwab, D.J., 1983. A two-dimensional lake circulation modeling system: programs to compute particle trajectories and the motions of dissolved substances. NOAA Technical Memorandum ERL GLERL-46, Great Lakes Environmental Research Laboratory. Ann Arbor, MI, p. 58 (PB83-257014).

Blumberg, A.F., Mellor, G.L., 1987. A description of a three-dimensional coastal ocean circulation model. In: Heaps, N.S. (Ed.), Three Dimensional Ocean Models, Coastal and Estuarine Sciences, 5. American Geophysical Union, Washington, DC, pp. 1–16.

Chan, C.H., Wiliams, D.J., Neilson, M.A., Harrison, B., Archer, M.L., 2003. Spatial and temporal trends in the concentrations of selected organochlorine pesticides (OCs) and polynuclear aromatic hydrocarbons (PAHs) in Great Lakes basin precipitation, 1986 to 1999. J. Great Lakes Res. 29 (3), 448–459.

Chapra, S.C., 1977. Total phosphorus model for the Great Lakes. J. Environ. Eng. Div. 103, 147–161.

Croley II, T.E., Hunter, T.S., 1994. Great Lakes monthly hydrologic data. NOAA Technical Memorandum ERL GLERL-83, Great Lakes Environmental Research Laboratory. Ann Arbor, MI, p. 83 (NTIS# PB95-173076/XAB).

DePinto, J.V., Young, T.C., McIlroy, M., 1986. Great Lakes water quality improvement: the strategy of phosphorus discharge control is evaluated. Environ. Sci. Technol. 20 (8), 752–759.

DiToro, D.M., and Connolly, J.P. 1980. Mathematical Models of Water Quality in Large Lakes, Part 2: Lake Erie. Report No. EPA-600/3-80-065, report to Large Lakes Research Station, ERL-Duluth, Grosse Ile, MI.

Dolan, D.M., 1993. Point source loadings of phosphorus to Lake Erie: 1986–1990. J. Great Lakes Res. 19 (2), 212–223.

DiToro, D.M., Thomas, N.A., Herdendorf, C.E., Winfield, R.P., Connolly, J.P., 1987. A post audit of a Lake Erie eutrophication model. J. Great Lakes Res. 13 (4), 801–825.

Dolan, D.M., McGunagle, K.P., 2005. Lake Erie total phosphorus loading analysis and update: 1996–2002. J. Great Lakes Res. 31 (Suppl. 2), 11–22.

Dolan, D.M., Yui, A.K., Geist, R.D., 1981. Evaluation of river load estimation methods for total phosphorus. J. Great Lakes Res. 7 (3), 207–214.

Gedney, R.T., Lick, W., 1972. Wind-driven currents in Lake Erie. J. Geophys. Res. 77, 2714–2723.

Hecky, R.E., Smith, R.E.H., Barton, D.R., Guildford, S.J., Taylor, W.D., Charlton, M.N., Howell, T., 2004. The nearshore phosphorus shunt: a consequence of ecosystem engineering by dreissenids in the Laurentian Great Lakes. Can. J. Fish Aquat. Sci. 61, 1285–1293.

Lam, D.C.L., Schertzer, W.M., McCrimmon, R.C., Charlton, M. and Millard, S. 2006. Modelling Phosphorus and Dissolved Oxygen Conditions Pre- and Post-*Dreissena* Arrival in Lake Erie. In: Munawar (ed), Pulse of Lake Erie, Aquatic Ecosystem Health and Management Society.

León, L.F., Imberger, J., Smith, R.E.H., Hecky, R.E., Lam, D.C.L., Schertzer, W.M., 2005. Modeling as a tool for nutrient management in Lake Erie: a hydrodynamics study. J. Great Lakes Res. 31 (Suppl. 2), 309–318.

Lesht, B.M., Fontaine, T.D., Dolan, D.M., 1991. Great Lakes total phosphorus model: post audit and regionalized sensitivity analysis. J. Great Lakes Res. 17 (1), 3–17.

Mellor, G.L., Yamada, T., 1982. Development of a turbulence closure model for geophysical fluid problems. Rev. Geophys. Space Phys. 20, 851–875.

Ohio Lake Erie Office, 1993. State of the Lake — 1992 Governor's Report on Lake Erie. Ohio Lake Erie Commission, Columbus, OH.

Rathke, D.E., McCrae, G., 1989. Appendix B, Volume III, Report of the Great Lakes Water Quality Board. International Joint Commission. Windsor, Ontario.

Saylor, J.H., Miller, G.S., 1987. Studies of large-scale currents in Lake Erie, 1979–80. J. Great Lakes Res. 13 (4), 487–514.

Task Group III (J.R. Vallentyne and N.A. Thomas, co-chairs), 1978. Fifth Year Review of Canada–U.S. Great Lakes Water Quality Agreement: Review of Phosphorus Loadings. IJC-Regional Office. Windsor, Ontario.

Tin, M., 1965. Comparison of some ratio estimators. J. Am. Stat. Assoc. 60, 294–307.

Vollenweider, R.A. 1968. The Scientific Basis of Lake and Stream Eutrophication, with Particular Reference to Phosphorus and Nitrogen as Eutrophication Factors. Technical Report DAS/DSI/68.27. Organization for Economic Cooperation and Development. Paris, France.

Vollenweider, R.A., 1976. Advances in defining critical loading levels for phosphorus in lake eutrophication. Mem. Ist. Ital. Idrobiol. 33, 53–83.